_		
1.Classification INPE.Co CDU: 523.4-852-36	2.Period  May 1979	4.Distribution Criterion
3.Key Words (selected by the author)		internal
Nitric oxide, Ion composition, Mesospheric temperature.		external $x$
5.Report No. INPE-1493-RPE/037	6.Date <i>May 1979</i>	7. Revised by
8. Title and Sub-title		9.Authorized by
DETERMINATION OF NITRIC OXIDE HEIGHT DISTRIBUTION FROM ROCKET ION COMPOSITION RESULTS AT LOW LATITUDES		Nelson de Jesus Parada Director
10.Sector DCE/DGA/GIO	Code <i>30.371</i>	11.No. of Copies <i>85</i>
12.Authorship M.A. Abdu		
Inez S. Batista		14.No. of Pages <i>16</i>
		15.Price
13.Signature of first author		
16.Summary/Notes  A detailed analysis is undertaken of ion composition results available from rocket measurements in the D and E region, using the presently known complete ion chemistry schemes, to determine the distribu-		

A detailed analysis is undertaken of ion composition results available from rocket measurements in the D and E region, using the presently known complete ion chemistry schemes, to determine the distribution of nitric oxide in this height region. The method of analysis uses, as input, an atmospheric model and the ion production rates due to X rays, and yields the heigh distribution of nitric oxide and production rates of the major initial ions  $NO^+$  (for a given Lyman a flux) and  $O_2^+$ . Analysis are carried out for Cassino (Brazil), a southern temperate latitude station and for Thumba, India, a northern low latitude station and the results are compared with available nitric oxide distributions from the  $NO_1$  band measurements. The role of the mesospheric water vapour and temperature on the deduced D region  $|NO_1|$  distribution is discussed.

17. Remarks This work was partially supported by "Fundo Nacional de Desenvolvimento Cientifico e Tecnológico (FNDCT)", Brasil, under contract FINEP-CT/130.

DETERMINATION OF NITRIC OXIDE HEIGHT DISTRIBUTION FROM ROCKET ION COMPOSITION RESULTS AT LOW LATITUDES

M.A. Abdu and Inez S. Batista

Instituto de Pesquisas Espaciais - INPE/Conselho Nacional de Desenvolvimento Científico e Tecnológico - CNPq, São José dos Campos, SP, Brasil

#### ABSTRACT

A detailed analysis is undertaken of ion composition results available from rocket measurements in the D and E region, using the presently known complete ion chemistry schemes, to determine the distribution of nitric oxide in this height region. The method of analysis uses, as input, an atmospheric model and the ion production rates due to X rays, and yields the height distribution of nitric oxide and production rates of the major initial ions  $\mathrm{NO}^+$  (for a given Lyman  $\alpha$  flux) and  $\mathrm{O_2}^+$ . Analyses are carried out for Cassino (Brazil), a southern temperate latitude station and for Thumba, India, a northern low latitude station and the results are compared with available nitric oxide distributions from the  $\mathrm{NO}$   $\gamma$  band measurements. The role of the mesospheric water vapor and temperature on the deduced D region [NO] distribution is discussed.

## INTRODUCTION

Considering the importance of Nitric Oxide, in the ionization balance of the lower ionosphere, very few direct measurements of its concentration has so far been obtained. This lack of information has, to some extent, slowed down our attempts to study such atmospheric processes as are involved in the seasonal, latitudinal and disturbed time variations in the lower ionospheric NO concentration. More

frequent and reliable determinations of [NO] is essential also for an understanding of the different ionization sources of the lower ionosphere on a global scale. Direct determinations from the rocket measurements of the NO  $\gamma$  band emission rates, [1,2], has uncertainties below about 90 km, though improved techniques have been introduced in more recent measurements [3,4]. Therefore, to complement the direct measurements, indirect determinations using ionospheric parameters such as electron density and ion composition, have been tried by several workers [5-10]. Indirect determinations of NO, especially those using the ion composition data, are fairly simple and reliable, above approximately 90 km, whereas at lower heights, where the process of conversion of the initial molecular ions,  $0^+_2$  and  $10^+$ , to their hydrates are important, reliable determination of the NO concentration would require involved calculation proceedures.

In the present paper, we have deduced the NO height distribution in the 80-110km region from the ion composition data measured by Narcisi et al. [11] over Cassino, Brazil on 5 November 1966, and by Aikin and Goldberg [12] over Thumba, India on 19 March 1970. The analysis is based on the presently known detailed ion chemistry for the lower ionosphere and the method of calculation, which uses as input, the ion composition data and the ion production rates due to X -rays in the 1-100Å band, yeilds the NO concentration and the production rates,  $q_{02}^+$  and  $q_{NO}^+$  of the major initial ions.

# Ion chemistry scheme

The number densities of NO<sup>+</sup> and O<sub>2</sub><sup>+</sup> and the total ion density,  $\Sigma N_1^+$ , measured in the lower ionosphere, in the present case from 80 to 110 km, are used to derive the NO density profile. NO<sup>+</sup> ions, in this height region, are produced by (1) photoionization of NO by the solar Lyman  $\alpha$  radiation and (2) charge transfer reaction,  $O_2^+ + NO \rightarrow NO^+ + O_2$ ; the  $O_2^+$  itself being produced by the ionization of  $O_2$  and  $O_2^+ \Delta g$  by the solar Lyman  $\beta$ , X radiation in the 1-100Å band and EUV. At the lower levels

of this height region, most of the  $\mathrm{NO}^+$  and  $\mathrm{O}_2^+$  produced are lost through three body reactions leading to the formation of the hydrates of these ions, before their dissociative recombination with electrons. The dissociative recombination becomes the important loss process of these ions only above, approximately, 90km. The cluster ion reaction path with  $0^{+}_{2}$  as the initial ion is generally more important at higher latitudes and under disturbed conditions. We have used the relevant reaction schemes and rate coefficients based on the works of Fehsenfeld and Ferguson [13], and Swider and Narcisi [14]. For the case of the low and middle latitude quiet D region, the more important reaction path in the 'cluster ion chemistry, is believed to be the one starting with NO as the initial ion. We have based this part of the reaction secheme on the recent works of Thomas [15] and Reid [16] that consider the three body reaction of  $\mathrm{NO}^+$  to form  $\mathrm{NO}^+.\mathrm{CO}_2$  and  $\mathrm{NO}^+.\mathrm{N}_2$ , the collisional dissociation of the latter two ions, and the switching reaction of the weakly bound NO . No with  ${
m CO_2}$  forming the more stable  ${
m NO}^+.{
m CO_2}$  as the initial stages in the production of NO+.H2O (besides the direct hydration of NO+), from which successive clustering proceeds. The complete reaction scheme, used in the analysis, is shown in Figure (1), and we may point out that hydration processes for either of the initial ions,  $0_2^{\dagger}$  or  $\mathrm{NO}^{\dagger}$ , are highly temperature dependent apart from their dependence on the mesospheric water vapor concentration.

# Method of deducing the NO density

Considering the reactions involving  $0_2^+$  and  $N0^+$  in the general scheme and assuming steady state, we can derive an expression for the equilibrium  $\left[N0^+\right]/\left[0_2^+\right]$  ratio. Since the full form of this expression obviously becomes fairly complicated, we give below a shorter representation of it, with a discussion of only the most essential aspects,

$$[NO^{+}]/[O_{2}^{+}] = \{(Q_{NO}^{+}/Q_{O_{2}^{+}})(L+D-M)+D\}/(F-G-H)$$
where 
$$Q_{NO}^{+} = q_{NO}^{+} + a_{1}[N_{2}^{+}] + b_{1}[N^{+}] + c_{1}[O^{+}]$$
and 
$$Q_{O_{2}^{+}} = q_{O_{2}^{+}} + a_{2}[N_{2}^{+}] + b_{2}[N^{+}] + c_{2}[O^{+}].$$

$$(1)$$

The description of the remaining simbols are same as in Abdu and Batista [10]. A second equation for the total ion density is written down as follows:

$$\Sigma N_{i}^{+} = (Q_{NO}^{+} + D[O_{2}])/(F-G-H) + Q_{O_{2}^{+}}/(L+D-M) + [N_{2}^{+}] + [N^{+}] + [O^{+}] + \Sigma^{m}[NO_{1}^{+}(H_{2}O)]_{i} + \Sigma^{m}[H^{+}.(H_{2}O)]_{j}$$
(2)

Since the cluster ions and ion hydrates can be calculated from NO<sup>+</sup> and O<sup>+</sup><sub>2</sub>, using an atmosphere model, the parameters that are considered unknown in the equations (1) and (2) are the nitric oxide concentration and the ion production rates. The  $\begin{bmatrix} N_2^+ \end{bmatrix}$ ,  $\begin{bmatrix} 0^+ \end{bmatrix}$  and  $\begin{bmatrix} N^+ \end{bmatrix}$  are directly related to their corresponding ion production rates  $q_{N_2^+}$ ,  $q_0^+$  and  $q_N^+$ . These ion production rates are due to X rays in the 1-100Å band and/or high energy charged particles, and, hence, they bear a fixed relationship among them and the corresponding  $q_{0_2^+}$ . Accordingly, for practical reasons, we divided the ion production rates into three groups: (a)  $q_{N_2^+}$  which is a function of NO density and the Lyman  $\alpha$  flux (taken for the present calculation as  $3 \times 10^{11}$  cm<sup>2</sup> sec<sup>-1</sup>), (b)  $q_{0_2^+}$  produced mostly by the action of solar Lyman  $\beta$  and EUV on  $q_{N_2^+}$  and  $q_{N_2^+}$  respectively, and (c)  $q_{N_2^+}$ ,  $q_0^+$ ,  $q_N^+$  and a fraction of  $q_{0_2^+}$ , all produced by X rays in the 1-100Å wavelength band. For the present analysis, we have adopted values for (c) from the results of Swider [17], and determined NO,  $q_{N_2^+}$  and  $q_{0_2^+}$  from equations (1) and (2).

According to the calculation procedure that we adopted, we first determined, from (1), an NO and  $q_{NO}^+$  that make the calculated  $\left[NO^+\right]/\left[O_2^+\right]$  ratio equal to that observed, and, subsequently,  $q_{O_2^+}$  was determined from (2) such that the observed  $\Sigma N_1^+$  was accounted for by the total ion production rates. Repetitions of the two steps of calculation were necessary, many times in some cases, to obtain the NO,  $q_{NO}^+$  that explain the observed  $\left[NO^+\right], \left[O_2^+\right]$  and  $\Sigma N_1^+$  simultaneously.

#### RESULTS AND DISCUSSION

The [NO] height profile deduced for Cassino, Brazil, from the ion composition results of Narcisi et al. [11], for a solar zenith angle  $\chi = 18^{\circ}$ , is presented in Figure 2 (above 106km the results are from extrapolated ion composition values and below 80km extrapolation of [NO] is done assuming constant mixing ratio). For

comparison, we have shown some experimental profiles from NO  $\gamma$  band measurements, over middle latitude at  $\chi$  = 63° by Meira[2] and around  $\chi$  = 90° by Tohmatsu and Iwagami [3], and by Baker et al. [4]. The morning result for Thumba, by Tohmatsu and Iwagami [3], is also shown. These various experimental profiles show very good agrement in their general features, especially in the occurrence of a minimum in NO density around 84 km. Our deduced NO distribution seems to agree with, though in general somewhat higher than, Meira's results above 86km, whereas the downward gradient on our profile, around this height, is steeper and [NO] below 84km is lower than in the experimental profiles. A well defined minimum near 84km, present in our result, is in excellent agreement with the experimental profile. Swider's [18] results, also deduced from the same ion composition results of Narcisi et al.(1972) for Brazil, show reasonably good agreement with ours above 85km. At 80km, his results, calculated by excluding the cluster ion chemistry, are, however, less than ours by a factor of 3. The same ion composition data was also used by Taubenheim [8] to deduce [NO] below 90km, but assuming a simplified model of the cluster ion chemistry, and his results show excellent agreement with ours above 85km, whereas, at lower heights, his results (not shown in the figure 2) are higher by factors of 3-5 than ours. The NO distribution, obtained by Mitra and Rowe [7] by applying constraints on the NO density profile which give best agreement between calculated ionization rates and the observed electron density profile, is also shown in figure 2, and it is generally higher than other results except near 80km. In figure 3 we have compared the results for Cassino, Brazil (30°S), with those for Thumba, India  $(8^{\circ}N)$ . Except in the height region 93-105km, there seems to be reasonably good agreement between the results for the case of  $\chi$  = 28°, for Thumba, and the results for Cassino, for which  $\chi$  is  $18^{\circ}$ . From the results shown for  $\chi$  =  $53^{\circ}$ , for Thumba, it may be observed that a possible zenith angle dependence of NO distribution seems to have oposite tendencies on either side of a transition region, which is around 92-95km. Taubenheim's [8] results, using the ion composition data of Goldberg and Aiken [19] below 87km, are also shown and there is good agreement

with our results near 86km.

Bellow 85km, the present analysis method offers a possibility to infer other atmosferic parameters such as the temperature or the water vapor concentration. The coefficeients used for the three body hydration reactions are highly temperature dependent (Reid [16], Swider and Narcisi [14], both for the forward reactions as well as for the collisional dissociation of the product. Further, the preffered hydration path depends upon the mesospheric water vapor concentration as well. Thus, we may observe that there could be a wide range of specific temperature and water vapor combinations that could yield NO values for an observed set of  $[NO^{+}]/[O_{2}^{+}]$  ratio and  $\Sigma N_{1}^{+}$ . When the water vapor profile of Shimazaki and Laird [20], shown in figure 4 (part a), is used, the corresponding temperature profile, required to obtain agreement between the observed and calculated results of  $[NO^{+}]$ ,  $[O_{2}^{+}]$  and  $\Sigma N_{1}^{+}$ , is shown in part (b) of the same figure. These temperatures are significantly higher than those used by Shimazaki and Laird in their modelling, shown also in part (b) of figure 4. Further, a reduction by an order of magnitude in the water vapor is not adequate to lower the required temperatures to the model values, shown in the figure 4. It seems, therefore, that the ion composition data over Cassino, is not consistent with the mesospheric temperature and water vapor models used over middle latitude, such as that given by Shimazaki and Laird [20]. Figure 5 presents, for 80, 82 and 86km, a more detailed relationship between the temperatures and water concentrations in their specific combinations, vapor that give agreement between the calculated and observed ion composition results, within about .1%. At 80 and 82km (and obviously for the lower levels, though not shown here), the relationship is well defined and is such that even a large uncertainty in  $m H_2O$ , in the lower concentration region along the respective curves, can still specify temperatures with reasonable accuracy. For large H<sub>2</sub>O concentrations, however, it becomes necessary to have more precise information on the water vapor concentration in order to infer the temperatures, and vice versa. The vertical bars, on the curve for 86km, show the variability in the required

temperatures for obtaining 1% agreement between the calculated and the observed ion composition data from which it is clear that, near this height and above, the process of matching the calculated and observed data becomes somewhat insensitive to the adopted temperature profile.

### CONCLUSIONS

We have used recket ion composition data for the lower ionosphere, in combination with the presently known detailed ion chemistry scheme, to deduce the Nitric oxide height distribution in this height region. The method of analysis, that utilizes the  $\left[\text{NO}^+\right]/\left[\text{O}_2^+\right]$  ratio and  $\left[\text{NN}_1^+\right]$ , yield, besides the  $\left[\text{NO}\right]$ , also the major ion production rates  $q_{\text{NO}}^+$  and  $q_{\text{O}_2^+}^+$ . The general features of the deduced NO profile, especially the occurrence of a minimum near 84km, agree very well with the experimental results from the NO  $\gamma$  band measurements. It appears that the determination of  $\left[\text{NO}\right]$ , using the detailed ion chemistry, can yield reliable results below 90km, where the determination from the NO  $\gamma$  band observation has still large uncertainty. It seems possible also to use the present method of analysis to infer other atmospheric parameters, such as the temperatures and water vapor concentrations in the mesosphere.

#### REFERENCES

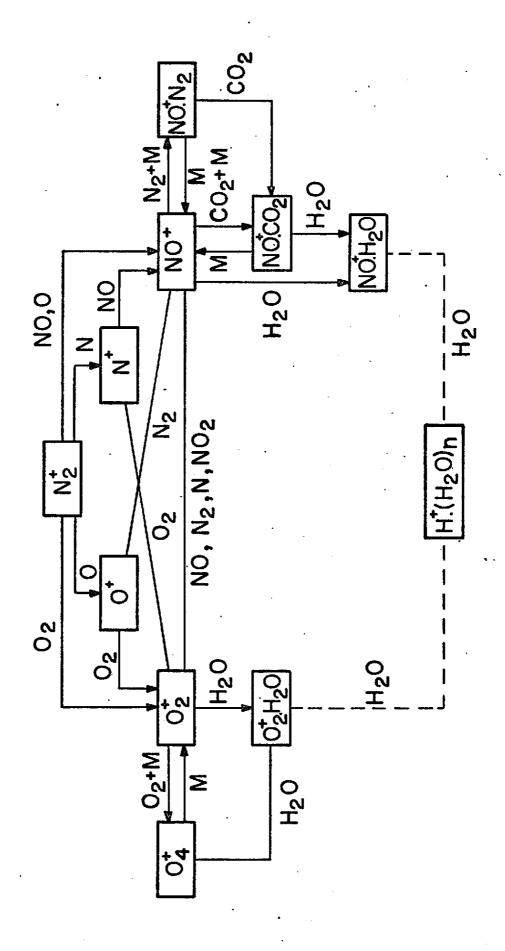
- 1. C. A. Barth, Ann. Geophys 22, 198 (1966)
- 2. L. G. Meira Jr., J. Geophys. Res 76, 202 (1971)
- 3. T. Tohmatsu and N. Iwagami, J. Geomag. Geoelectr. 28,343 (1976)
- 4. K. D. Baker, A. F. Nagy, R. D. Olsen and E. S. Oran, <u>J. Geophys. Res.</u> 82,3281 (1977)
- 5. A. P. Mitra, J. Atmos. Terrest. Phys. 28,945 (1966)
- 6. R. S. Narcisi, C. R. Philbrick, J. C. Ulwick and M. E. Gardner, <u>J. Geophys.</u>
  Res. 77, 1332 (1972)
- 7. A. P. Mitra and J. N. Rowe, <u>J. Atmos. Terrest. Phys.</u> 36, 1707 (1974)
- 8. J. Taubenheim, Space Research XVII, 271 (1977)

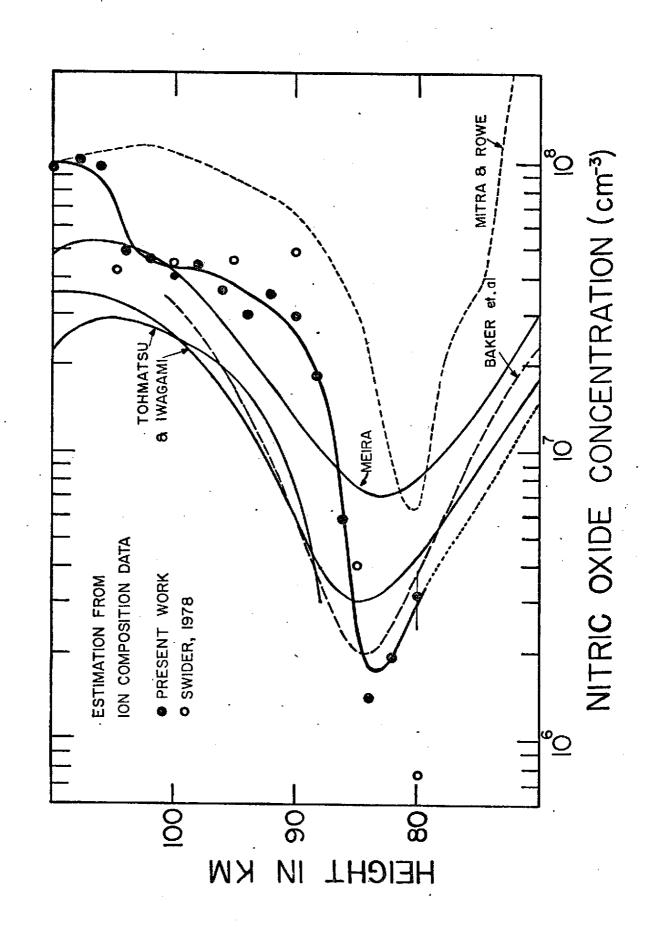
- 9. W. Swider, <u>J. Geophys</u>. <u>Res. 83</u> 4407 (1978)
- 10. M. A. Abdu and I. S. Batista, J. Geophys. Res. in press.
- 11. R. S. Narcisi, A. D. Bailey, L. E. Wlodyka and C. R. Philbrik, <u>J. Atmos.</u>

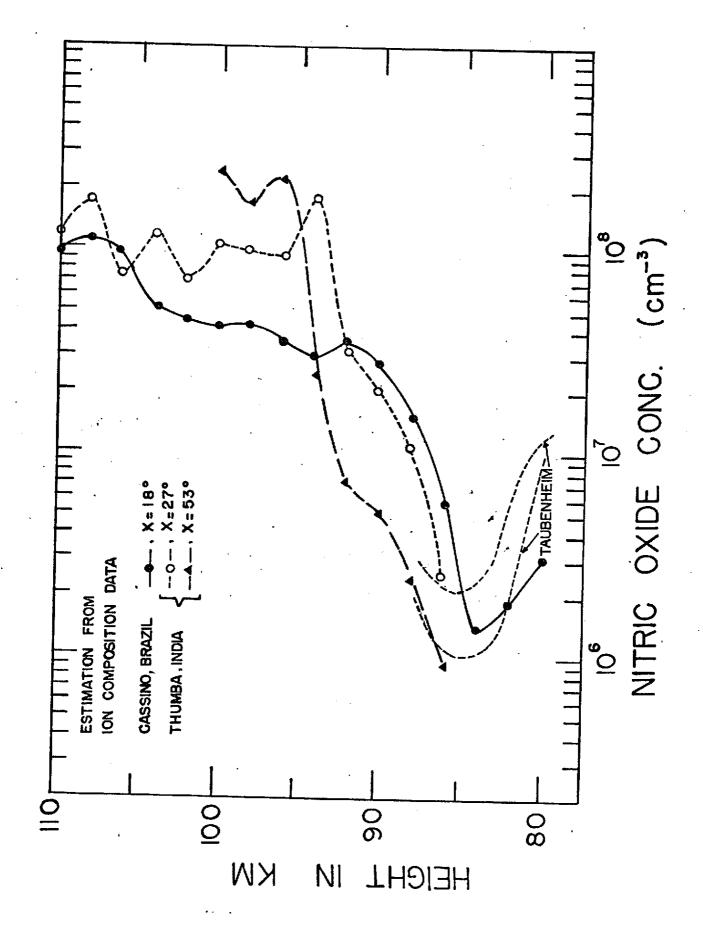
  Terrest. Phys. 34, 647 (1972)
- 12. A. C. Aikin and R. A. Goldberg, <u>J. Geophys. Res.</u> <u>78</u>, 734 (1973)
- 13. F. C. Fehsenfeld and E. E. Ferguson, <u>J. Geophys. Res.</u> 74, 2217, (1969)
- 14. W. Swider and R. S. Narcisi, <u>J. Geophys. Res.</u> <u>80</u>,655 (1975)
- 15. L. Thomas, <u>J. Atmos. Terrest. Phys.</u> 38,61 (1976)
- 16. G. G. Reid, Planet. Space Sci. 25,275 (1977)
- 17. W. Swider, Rev. Geophys. 7, 573 (1969)
- 18. W. Swider, J. Geophy. Res. 83, 4407 (1978)
- 19. R. A. Goldberg and A. C. Aikin, Aeronomy Rep. No. 48, Univ. of Illinois, 160, (1972)
- 20. I. Shimazaki and A. R. Laird, Radio Sci. 1, 23 (1972)

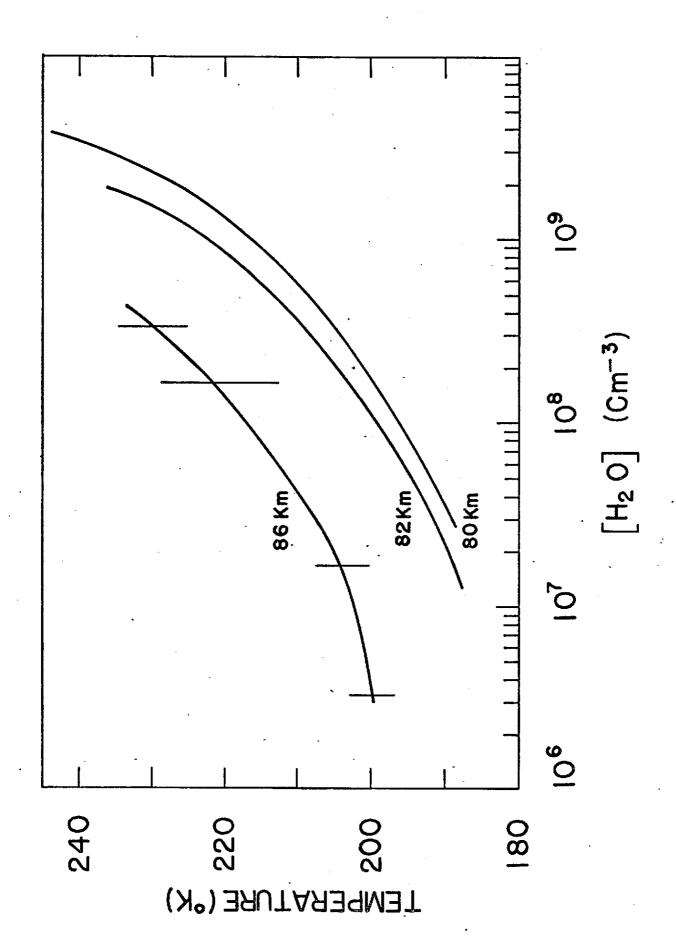
#### FIGURE CAPTIONS

- Figure 1. Ion chemistry scheme used in the analysis.
- Figure 2. Nitric oxide height distribution for Cassino, Brazil, obtained from the present analysis, compared to some experimental profiles from NO  $\gamma$  band measurement and indirect determinations from ionospheric parameters. The results of the present analysis are shown by points at intervals of 2km, through which a smooth profile is drawn.
- Figure 3. A comparison of the NO height distribution deduced from ion composition data for Cassino. Brazil and Thumba, India. The part of the curves below 87km (shown broken) for Thumba, was taken from Taubenheim (1977).
- Figure 4. The temperature and water vapor profiles used in the analysis. The temperature curve indicated as 'present result' was used with  $\rm H_2O$  profile of Shimazaki and Laird shown in part (a). The temperatures indicated by the solid triangles corresponds to  $\rm [H_2O]$  reduced by 10 times.
- Figure 5. Relationship between temperatures and  $[H_20]$  that gave agreement, within 0.1%, between the calculated and observed ion density data, plotted for 80km, 82km and 86km.









ir.

